Learning-based Distributed Approach to Energy-optimized Speed Trajectory for Electric Vehicles at Multiple Signalized Intersections

Yuki Hosomi, Binh-Minh Nguyen, Sakahisa Nagai, Hiroshi Fujimoto
The University of Tokyo
5-1-5, Kashiwanoha, Kashiwa, Chiba, 277-8561, Japan
Corresponding author's e-mail: hosomi.yuki22@ae.k.u-tokyo.ac.jp

***Abstract*—Range extension via speed trajectory optimization is an important issue for battery electric vehicles (EVs). To this end, this paper contributes a practical approach to globally minimize the energy consumption of EVs passing through multiple signalized intersections. The energy consumption is estimated using a traffic flow Gaussian mixture model (GMM) obtained from floating car data. Then, the optimal speed trajectory is generated using dynamic programming (DP). The algorithm is solved distributedly for each segment between two adjacent intersections, thereby, alleviating the computational burden. Furthermore, the proposal does not require vehicle-to-vehicle (V2V) and vehicle-to-infrastructure (V2I) communication. Experimental results demonstrate that the proposed algorithm can successfully reduce energy consumption. The reductions are respectively 11.7% and 8.0% compared to the simple strategy with the constant speed and acceleration/deceleration, and the conventional method which independently minimizes the energy consumption in each road segment between two adjacent intersections.**

***Index Terms*—electric vehicle, energy minimization, floating car data, Gaussian mixture model, multiple signalized intersections, speed trajectory optimization.**

I. Introduction

EVs have been attracting more and more attention around the world. Although EVs have a remarkable merit of fast and accurate torque response [1], the short mileage per charge is their major challenge. To overcome this problem, cruising range extension by optimizing the use of electric energy has been tackled from various points of view. Typical examples are range extension control via motor torque/driving force distribution [2], [3] and energy management [4], [5].

As the vehicle speed has a significant impact on energy consumption, the focus of this paper is speed trajectory optimization (STO) for EVs. From a literature review, this issue can be solved by different methods, which vary due to the constraint scenarios of the optimization problem. For instance, STO for solar vehicles is proposed [6]. For another example, considering the preceding vehicle velocity, STO for ecological adaptive cruise control can be realized via quadrant dynamic programming [7]. These studies are mainly for highways. On the other hand, for urban road systems, many STO methods considering traffic signals have been proposed. However, the existing STO methods have the following issues.

Some previous methods proposed STO for multiple signalized intersections [8], [9]. The optimization in [8] was solved in a centralized way by taking into account all the road segments. However, due to the computational burden, this is not suitable for a road including a large number of intersections. In some studies, machine learning is used for online optimization [9]. However, the computational burden of onboard computers is still at a high level.

Most previous methods rely on V2I, however, it takes time for connected and automated vehicles to spread [10]. In addition, it is essential to note that the cycle and offset time of some traffic signals are frequently adjusted to achieve smooth traffic flow [11]. With respect to this scenario, learning-based traffic signal estimation is important for more practical STO. For instance, even in the case of using V2I or V2V, previous methods utilized data-driven probabilistic parameters to consider the uncertainty of information [12], [13]. Furthermore, the STO for combustion engine vehicles without V2I was developed based on the probability of passing the next traffic signal, which can be estimated from a Gaussian process regression using self-driving data [14], [15]. Recently, by utilizing the floating car data collected by the ETC2.0 system [16], we presented a STO method for EVs operating a single road segment with only two traffic signals [17]. However, it is still necessary to extend to deal with multiple signalized intersections.

Based on the above discussion, this paper aims to contribute a new STO method for EVs operating between multiple signalized intersections. For more practical uses, the proposal does not rely on the V2I or V2V. The method consists of two stages. In the first stage, the energy consumption of EVs operating on N-road-segment is predicted by using stochastic traffic flow models (GMM). In the second stage, the estimated energy and probability are used to optimize the speed trajectory to the next traffic signal via DP. Unlike the centralized algorithm [8], the proposed algorithm is solved in a distributed way for each road segment. Unlike [9], the learning algorithm from floating car data is only used for offline calculation of the GMM. This reduces the computational burden and enables the practical implementation of the proposal. This study focuses on low-speed urban road conditions with coordinated controlled traffic signals. The proposed method is developed based on the battery EV prototype, which is driven by front in-wheel motors (IWMs) of permanent magnet synchronous types.

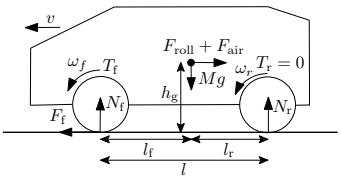

Fig. 1. Longitudinal model of an EV with front IWMs.

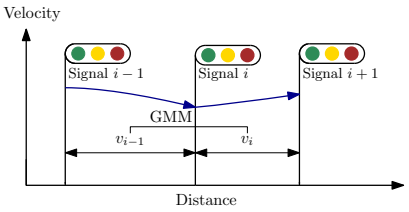

Fig. 2. Average speed definition for GMM.

II. Modeling

A. Energy Consumption Model

This study considers the longitudinal motion of EVs with front IWMs which is described in Fig. 1. The equations that describe the rotational motion of the wheel and the motion of the vehicle are expressed as

$$J_\omega \frac{d\omega_\#}{dt} = T_\# - rF_\#, \ \# = \{\mathrm{fl}, \ \mathrm{fr}\}, \tag{1}$$

$$M\frac{dv}{dt} = F_{\mathrm{fl}} + F_{\mathrm{fr}} - F_{\mathrm{DR}}, \tag{2}$$

where J_ω, $T_\#$, $F_\#$, F_{DR}, v, ω_h, r, and M are the wheel's moment of inertia, motor torque, driving force, dragging force, vehicle speed, wheel speed, wheel radius, and vehicle mass, respectively. The subscript $\#$ means the position of the IWM; fl and fr are front-left and front-right, respectively.

The driving force $F_\#$ is defined as (3) by the slip ratio $\lambda_\#$ and the load force of front N_{f}. The dragging force is given as (4), which is the sum of air resistance and rolling resistance.

$$F_\# \simeq N_{\mathrm{f}} D_{\mathrm{s}} \lambda_\#, \tag{3}$$

$$F_{\mathrm{DR}} = \mu_{\mathrm{r}} Mg + b|v| + F_{\mathrm{a}} v^2, \tag{4}$$

D_{s}, μ_{r}, b, and F_{a} are the driving stiffness coefficient, rolling resistance coefficient, viscous resistance coefficient, and air resistance coefficient, respectively.

Energy consumption is estimated from the torque and wheel speed. In this study, the inverter loss and the mechanical loss of the motor are neglected, thus the input power P_{in} is the sum of output power P_{out}, copper loss P_{cu}, and iron loss P_{fe}. Considering the permanent magnet synchronous motor types, the aforementioned powers are formulated as

$$P_{\mathrm{in}} = P_{\mathrm{out}} + P_{\mathrm{cu}} + P_{\mathrm{fe}}, \tag{5}$$

$$P_{\mathrm{out}} = \sum_{\mathrm{all}} \omega_\# T_\# \simeq 2\frac{v}{r} T_\#, \tag{6}$$

$$P_{\mathrm{cu}} = \sum_{\mathrm{all}} R \left(\frac{T_\#}{K_t}\right)^2, \tag{7}$$

$$P_{\mathrm{fe}} = \sum_{\mathrm{all}} \frac{(\omega_\# p_{\mathrm{n}})^2}{R_c} \left(L_q^2 \left(\frac{T_\#}{K_t}\right)^2 + \Psi^2 \right), \tag{8}$$

where K_t, p_{n}, R, L_q, Ψ, and R_{c} are the motor torque coefficient, number of pole pairs, copper loss resistance, q-axis inductance, leakage flux, and equivalent iron loss resistance, respectively. The formula (8) is derived under the assumption that the d-axis current is very small in comparison with the q-axis current [3].

Assuming that the slip ratio is small, the wheel speed is approximated by the vehicle speed. Thus, the energy can be seen as a function of vehicle speed.

B. Learning-based Traffic Flow Model

A traffic flow GMM model is generated from floating car data to consider traffic signal constraints. The GMM G is the sum of n two-dimensional Gaussian distributions g with the average speed represented by X [17].

$$G = \sum_{k=1}^{n} \pi_k g_k \tag{9}$$

$$g_k = (2\pi|\Sigma_k|)^{-\frac{1}{2}} e^{\{(-\frac{1}{2})(X-\mu_k)^T \Sigma_k^{-1}(X-\mu_k)\}} \tag{10}$$

$$X = [v_{i-1} \ v_i]^{\mathsf{T}} \tag{11}$$

μ_k, Σ_k, and π_k are the mean, variance, and mixing coefficient, respectively. As shown in Fig. 2, v_i is defined as the average speed between the signal $i-1$ and signal i which is estimated from floating car data. Assuming the use of low-frequency data, the average speeds that can be estimated even from low-frequency data are chosen as the variables.

To obtain the probability distribution of v_i when v_{i-1} is given, the probability ρ is normalized by the total probability of v_{i-1} as shown in the following equation.

$$\rho(v_i \mid v_{i-1}) = \frac{\int_{v_i-\Delta v}^{v_i+\Delta v} \int_{v_{i-1}-\Delta v}^{v_{i-1}+\Delta v} G dv_{i-1} dv_i}{\int_{v_{i,min}}^{v_{i,max}} \int_{v_{i-1}-\Delta v}^{v_{i-1}+\Delta v} G dv_{i-1} dv_i}, \tag{12}$$

where Δv is the discretization step.

III. Speed Trajectory Generation Method

A. Problem Setting

For each traffic signal on the route, a prediction horizon and a control horizon are defined. In the prediction horizon, energy consumption $\hat{W}'_{i,i+1}$ is predicted using GMM and DP, and in the control horizon, the energy-efficient speed trajectory v_l is generated by DP using $\hat{W}'_{i,i+1}$ and the probability distribution of v_i. The following optimization problem for energy minimization is solved successively for all traffic signals $i = \{0, 1, \cdots, N_{\mathrm{all}}\}$ on the route.

$$\min_{v(l)} \ E\left[\sum_{l=0}^{L} (P_{\mathrm{in}}(v(l))\Delta t + \alpha \Delta t) + \hat{W}'_{i,i+1}(\hat{v}_i)\right] \tag{13}$$

$$\text{s.t.:} \quad \hat{W}'_{i,i+1}(\hat{v}_i) = \sum_{j=1}^{N-1} w_{i+j}(\hat{v}_{i+j-1}), \tag{14}$$

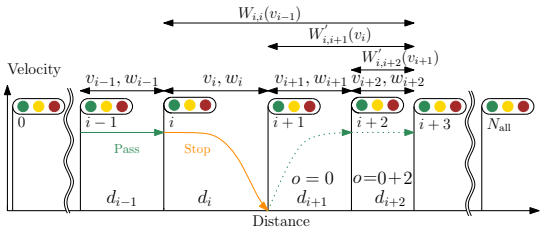

Fig. 3. Variable definitions for multiple signals.

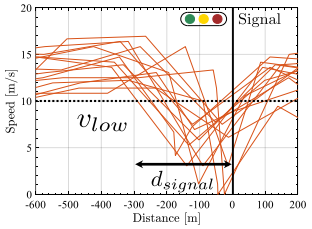

Fig. 4. Example of v_{low} and d_{signal} obtained from ETC2.0 probe data.

where l, L, N_{all}, N, α, and Δt are the time step and the terminal time of the control horizon, the number of traffic signals of the entire route and the prediction horizon, the accessory power, and sample time of DP, respectively. The distance d_i, and energy consumption w_i are defined as shown in Fig. 3.

It is assumed that the route is determined before driving and the location of the traffic signals can be known in advance from the map. Uncongested road environments are assumed, and constraints of surrounding vehicles are not considered. GMM is used to consider the uncertainty of traffic signal period and offset time. It is reasonable to assume that the onboard system detects traffic signals within a certain distance from the vehicle and determines if it can pass through. In addition, for the optimization, d_{signal} and v_{low} are given from the floating car data. As shown in Fig. 4, d_{signal} means the distance for deceleration in front of a traffic signal, and v_{low} means the lowest cruising speed.

B. Proposed Algorithm

Fig. 5 shows the flowchart of the proposed STO algorithm consisting of two stages: an offline estimation of the energy consumption through the prediction horizon of each traffic signal and an online STO to the next traffic signal. In the first stage, the energy consumption $w_i(v_{i-1}, v_i)$ is estimated for each pair of v_{i-1} and v_i. Adding up the product of energy w and probability ρ, the expected energy consumption of the entire prediction horizon $W_{i,i}(v_{i-1})$ is estimated. In the next online stage, the speed trajectory is optimized based on the probability distribution of $\hat{v}_i$ and the terminal cost of the expected energy consumption $W'_{i,i+1}(\hat{v}_i)$. The boundary condition of the optimization problem depends on whether the vehicle passes through signal i or not. The online STO is repeated each time the vehicle passes through a traffic signal on its route.

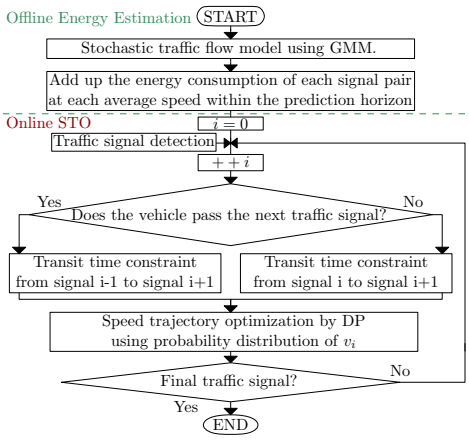

Fig. 5. Flowchart of the proposed algorithm.

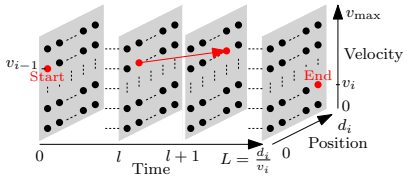

Fig. 6. DP table.

C. Offline Energy Estimation

In this subsection, the total energy consumption W_i is obtained by adding up the energy consumption on each road segment between a pair of two consecutive signals.

1) Energy Estimation of Each Traffic Signal Pair: The expected energy of each road segment is estimated as the product of the probability from GMM and the energy from DP. Energy is obtained from the pre-computed DP tables by defining the boundary conditions as shown in Fig. 6. $\mathrm{DP}(v_{ini}, v_{ter}, T, d)$ means the energy calculated from the DP table when v_{ini}, v_{ter}, T, and d are given as the initial speed, terminal speed, total time, and distance. The cases are classified by v_i to properly estimate deceleration and stop before the signal. If $v_i \geq v_{low}$, the energy consumption of ith segment is estimated from the following equation.

$$w'_i(v_{i-1}, v_i) = \mathrm{DP}\left(v_{i-1}, v_i, \frac{d_i}{v_i}, d_i\right) \tag{15}$$

On the other hand, if $v_i < v_{low}$, it is assumed that the vehicle decelerates or stops in front of signal $i+1$. Thus, the section is divided into two parts: a subsection with constant speed $v_{con} = \max(v_{i-1}, v_{low})$, and another with a stop in front of signal $i+1$. The energy consumption can be expressed by the following equation.

$$w'_i(v_{i-1}, v_i) = \mathrm{DP}\left(v_{i-1}, v_{con}, \frac{d_i - d_{signal}}{v_{con}}, d_i - d_{signal}\right) + \mathrm{DP}\left(v_{i-1}, v_i, \frac{d_i}{v_i} - \frac{d_i - d_{signal}}{v_{con}}, d_{signal}\right) \tag{16}$$

From the above, the expected energy consumption of each traffic signal segment is calculated from w and ρ. The expected

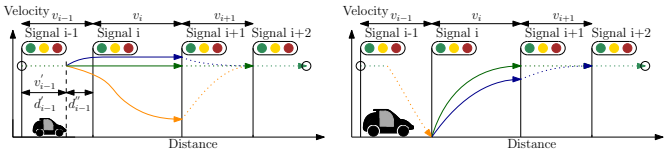

(a) Possible pass trajectories. (b) Possible stop trajectories.

Fig. 7. Optimization section and speed trajectory.

energy for all possible v_{i-1} is obtained by summing expected energy for all average speed v_i at each v_{i-1}, as

$$w_{i,o}(v_{i-1}) = \sum_{k=0}^{K} w_i^{'}(v_{i-1}, k\Delta v)\rho_{i,o}(v_{i-1}, k\Delta v), \tag{17}$$

$$K = \text{round}\left(\frac{v_{\max}}{\Delta v}\right), \tag{18}$$

where o means the index that identifies GMMs with different training floating car data according to the passing and stopping of traffic signals that are located before the target signal.

2) Energy Estimation of Entire Route: By adding up the expected energy w, the energy consumption of the entire prediction horizon W_i is estimated. Energy consumption is calculated sequentially starting from the terminal signal pair. There are 2^{N-1} GMMs at the terminal signal pair of the prediction horizon that are derived from various floating car data classified by passing and stopping. If $v_i < v_{low}$, the vehicle is considered to have stopped at signal $i+1$.

$$W_{i,N,o}^{'}(v_{N-1}) = w_{N,o}(v_{N-1}) \tag{19}$$

$$o = \sum_{j=1}^{N-1} \xi_j 2^{j-1} = \{o \in \mathbb{Z} \mid 0 \le o \le 2^{N-1} - 1\} \tag{20}$$

$$\xi_j = \begin{cases} 0 & \text{if } v_{j-1} \ge v_{low} \\ 1 & \text{if } v_{j-1} < v_{low} \end{cases} \tag{21}$$

The above calculation is applied to other traffic signals from behind. The energy of the next traffic signal pair is added to the terminal cost. The terminal cost is determined by v_{j-1} considering both the passing and stopping situations.

$$W_{i,j,o}^{'}(v_{j-1}) = w_{j,o}(v_{j-1}) + \begin{cases} W_{i,j+1,o}^{'}(v_{j,k}) & \text{if } v_{j-1} \ge v_{low} \\ W_{i,j+1,o+2^{j-1}}^{'}(v_{j,k}) & \text{if } v_{j-1} < v_{low} \end{cases} \tag{22}$$

$$o = \{0, 1, 2, \cdots, 2^{j-1} - 1\} \tag{23}$$

$$j = \{N + i - 1, N + i - 2, \cdots, 1\} \tag{24}$$

Finally, $W_{i,i}(v_{i-1})$ is obatined.

D. Online STO

As the final step, DP generates speed trajectories to signal $i+1$ when traveling between signal $i-1$ and i. The estimated energy consumption of the prediction horizon is added to the objective function for the separation and nonseparation cases of the probability distributions [17]. The boundary conditions depend on the passing and stopping of signal i.

When passing through signal i, Fig. 7(a) shows the possible speed trajectory. The initial position is the point where the vehicle detects signal i, and the terminal point is at signal $i+1$. To optimize the transit time from signal $i-1$ to signal $i+1$, the combination of v_{i-1} and v_i is optimized. Using GMM, v_{i-1} is optimized based on the expected energy consumption $W_{i,i}$ and the energy consumption for speed change from $v_{i,ini}$ to v_{i-1}.

$$\min_{v_{i-1}} W_{i,i}(v_{i-1}) + \text{DP}\left(v_{i,ini}, v_{i-1}, \frac{d_{i-1}^{''}}{v_{i-1}}, d_{i-1}^{''}\right) \tag{25}$$

On the other hand, when stopping at signal i, the possible speed trajectory is shown in Fig. 7(b). The initial and terminal position is at signal i and $i+1$, respectively. To obtain the probability distribution of v_i, v_{i-1} is calculated from driving data.

The generation strategies for the case when the probability distributions separate and the case when they do not separate are shown below:

1) Case 1: Probability Distribution Separates: The optimization problem in the case of separate probability distributions is expressed as

$$\min_{v(l),\hat{v}_i} E\left[\sum_{l=0}^{L}(P_{\text{in}}(v(l))\Delta t + \alpha\Delta t) + \phi(\hat{v}_i)\right], \tag{26}$$

$$\text{s.t.:} \quad \hat{v}_i = \{\hat{v}_{\text{pass}}, \hat{v}_{\text{stop}}\}, \tag{27}$$

$$\begin{cases} \begin{cases} L = \text{round}\left(\frac{d_i}{\hat{v}_i \Delta t}\right), \\ \phi(\hat{v}_i) = W_{i,i+1,0}^{'}(\hat{v}_i), \qquad \text{if } v_{i-1} \ge v_{low} \\ x(0) = 0,\ x(L) = d_i, \end{cases} \\ \begin{cases} L = \text{round}\left(\frac{d_{i-1}}{v_{i-1}\Delta t} + \frac{d_i}{\hat{v}_i \Delta t} - \frac{v_{i-1}^{'}}{d_{i-1}^{'}\Delta t}\right), \\ \phi(\hat{v}_i) = W_{i,i+1,1}^{'}(\hat{v}_i), \qquad \text{if } v_{i-1} < v_{low} \\ x(0) = d_{i-1}^{'},\ x(L) = d_{i-1} + d_i, \end{cases} \end{cases} \tag{28}$$

$$v(0) = v_{i,ini},\ v(L) = \hat{v}_i, \tag{29}$$

$$x(k+1) = x(k) + \frac{v(k+1) + v(k)}{2}\Delta t, \tag{30}$$

$$T_{\min} \le T(k) \le T_{\max}, \tag{31}$$

where $\hat{v}_{\text{pass}}$, and $\hat{v}_{\text{stop}}$ are the assumed pass and stop average speeds, respectively. Both average speeds are defined as the expected values of each separated probability distribution of v_i. The expected energy consumption of the future section is added to the cost function, thus DP can optimize the speed trajectory while also taking into account the traffic signals ahead.

2) Case 2:Probability Distribution Does Not Separate: Energy optimization problems are given below in the case of non-separable probability distributions. The difference is that the average speed is optimized on one dimension.

$$\min_{v(l),\hat{v}_i} E\left[\sum_{l=0}^{L}(P_{\text{in}}(v(l))\Delta t + \alpha\Delta t) + \phi(\hat{v}_i)\right] \tag{32}$$

$$\text{s.t.:} \quad (28) - (31) \tag{33}$$

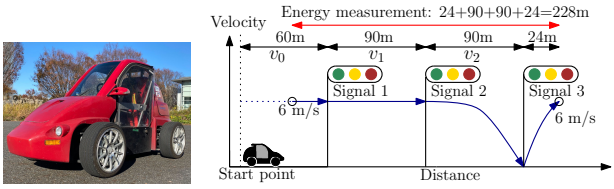

(a) FPEV2-Kanon. (b) Road with multiple intersections.

Fig. 8. Experimental electric vehicle and road settings.

TABLE I
VEHICLE SPECIFICATION.

Parameter	Value
M	925 kg
μ_r	0.01
b	15.4 kg/s
F_a	0.047 $\mathrm{Ns}^2/\mathrm{m}^2$
$J_{\omega\mathrm{f}}$	1.24 kgm^2
D_s	10

TABLE II
IWM SPECIFICATION.

Parameter	Value
L_q	0.000 69 mH
Ψ	0.18 Wb
R	0.06 Ω
p_n	10
K_t	1.8 Nm/A
r	0.301 m

IV. EVALUATION

A. Evaluation Setting

To evaluate the proposed method, an experimental vehicle FPEV2-Kanon driven by front-IWMs is used (Fig. 8(a)). The main parameters of the vehicle and the IWM are summarized in Tables I and II, respectively.

For evaluation, this paper compares the proposed method (Prop.) with the conventional method (Conv.) which considers only the single traffic signal segment [17] and the constant speed and acceleration/deceleration trajectory (Const.) of $6\,\mathrm{m/s}$ and $1\,\mathrm{m/s}^2$ without using an optimization algorithm. $6\,\mathrm{m/s}$ is the energy-optimized speed for constant speed operation considering accessory power ($\alpha = 600\,\mathrm{W}$). This study assumes an urban traffic environment such as the WLTC driving cycle's low mode. Due to the constraints of the experimental field, a road segment with three intersections is used for verification. The distances between intersections are both $90\,\mathrm{m}$. For evaluation, the inverter input power is measured as P_in, and the accessory loss is calculated from the running time. The total energy is the sum of the inverter power and the accessory power to run $228\,\mathrm{m}$ as shown in Fig. 8(b).

It is assumed that the signal condition could be detected from $d_{signal} = 24\,\mathrm{m}$, and the vehicle controller decides to pass or stop. The learning data for GMM is generated by a constant acceleration/deceleration trajectory with no prior signal information. This is to simulate ordinary human driving behavior. It is assumed that the starting time to approach Signal 1 is random. The prediction horizon when generating speed trajectories to Signal 2 is from Signal 2 to Signal 3.

For optimization of DP, time and speed are discretized by $0.5\,\mathrm{s}$ and $0.125\,\mathrm{m/s}$, respectively. Optimal speed trajectories are generated and given to the experimental vehicle, which is controlled by a combination of a PI controller and a FF controller. Only regenerative braking is used for deceleration.

The simulation verifies the case when the offset time between traffic signals varies stochastically from $-2.5\,\mathrm{s}$ to $2.5\,\mathrm{s}$ randomly with a uniform distribution, while the experiment verifies the situations when the offset time fixed at $0\,\mathrm{s}$.

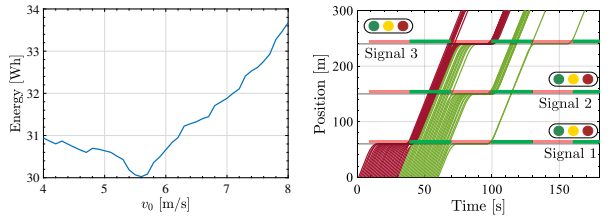

(a) Expected energy at each v_0. (b) Vehicle trajectories of Const.

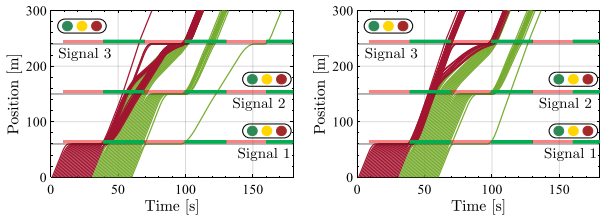

(c) Vehicle trajectories of Conv. (d) Vehicle trajectories of Prop.

Fig. 9. Simulation results. Offset time varies stochastically.

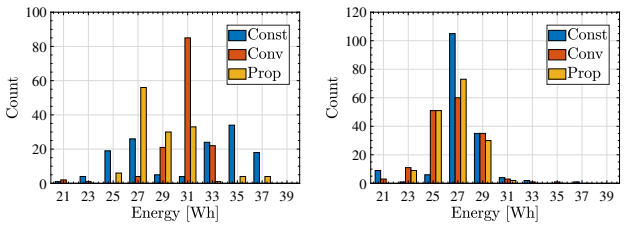

(a) Expected energy consumption when stopping at Signal 1. (b) Expected energy consumption when passing through Signal 1.

Fig. 10. Energy consumption (simulation).

B. Stochastic Simulation

In the stochastic simulations, 300 simulation trials are performed for each method for energy consumption comparison. Fig. 9(a) is the estimated expected energy at each v_0 when $v_{0,ini} = 6\,\mathrm{m/s}$, and it indicates that $v_0 = 5.6\,\mathrm{m/s}$ is the energy-optimized speed.

The vehicle trajectories of Const., Conv., and Prop. are shown in Figs. 9(b), 9(c), and 9(d), respectively. The color of the line indicates the status of Signal 1 when the vehicle reaches it. Vehicles using Conv. and Prop. methods can decelerate after Signal 2 when passing through both Signals 1 and 2. Notably, the proposed method allows some vehicles to accelerate and pass through Signal 3 after stopping at Signal 1. This operation is impossible by using the conventional method. On the other hand, when passing through Signal 1, energy reduction by the proposed method is small due to the low accuracy of passage time. Figs. 10(a) and 10(b) show the energy consumption distribution. Table III shows the expected energy of the simulation. Although there are cases where the use of the proposed method increases the energy, the expected energy consumption of Prop. can be reduced by $5.2\,\%$ and $2.9\,\%$ compared to Const. and Conv., respectively.

TABLE III
EXPECTED ENERGY CONSUMPTION COMPARISON.

Method	Simulation		Experiment	
	Stop Signal 1	Pass Signal 1	Stop Signal 1	Pass Signal 1
Const.	30.7 Wh	27.5 Wh	30.4 Wh	24.4 Wh
Conv.	30.2 Wh	26.6 Wh	28.1 Wh	24.5 Wh
Prop.	28.8 Wh	26.4 Wh	23.9 Wh	24.5 Wh

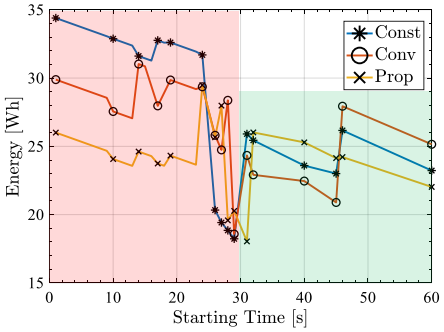

Fig. 11. Energy consumption (experiment). The background color corresponds to the traffic signal color when the vehicle reaches Signal 1.

C. Experimental Results

Fig. 11 demonstrates the energy consumption of the Const., Conv., and Prop. for some starting time from 0 to 60 s. Table III shows the expected energy consumption. Energy consumption is reduced in both cases when passing through and stooping at signal 1, and overall the proposed method reduces energy consumption by 11.7 % and 8.0 % compared to Const. and Conv., respectively. The vehicle trajectories in the experiment are almost the same as in the simulation. In the experiment, the uncertainty of the offset time is small, therefore the proposed method using learning is more effective.

V. CONCLUSION

This study proposed a learning-based distributed stochastic energy-minimization method that can be applied to multiple signalized intersections without using V2I. The optimal average speed is obtained by predicting the expected energy by GMM obtained from floating car data. The expected energy is introduced as a terminal cost to generate speed trajectories between adjacent intersections. The proposed method is shown to be suitably adapted to multiple intersections, as it alleviates the computation burden. Stochastic simulation and experiments show that the proposed method reduces the expected energy. Moreover, the proposed method can be straightforwardly extended to other EV prototypes. In the future, we aim to extend online optimization by using model predictive control considering additional constraints given by the preceding vehicle.

ACKNOWLEDGMENT

This research was partly supported by Kashiwa ITS Promotion Council including Kanto Regional Development Bureau of the Ministry of Land, Infrastructure, Transport, and Tourism.

REFERENCES

[1] T. Suzuki, M. Mae, T. Takeuchi, H. Fujimoto, and E. Katsuyama, "Model-based filter design for triple skyhook control of in-wheel motor vehicles for ride comfort," *IEEJ Journal of Industry Applications*, vol. 10, no. 3, pp. 310–316, 2021.

[2] S. Harada and H. Fujimoto, "Range extension control system for electric vehicles during acceleration and deceleration based on front and rear driving-braking force distribution considering slip ratio and motor loss," in *IECON 2013 - 39th Annual Conference of the IEEE Industrial Electronics Society*, 2013, pp. 6626–6631.

[3] Y. Ikezawa, H. Fujimoto, Y. Hori, D. Kawano, Y. Goto, M. Tsuchimoto, and K. Sato, "Range extension autonomous driving for electric vehicles based on optimal velocity trajectory generation and front-rear driving-braking force distribution," *IEEJ Journal of Industry Applications*, vol. 5, no. 3, pp. 228–235, 2016.

[4] M. Naguib, P. Kollmeyer, and A. Emadi, "Application of deep neural networks for lithium-ion battery surface temperature estimation under driving and fast charge conditions," *IEEE Transactions on Transportation Electrification*, vol. 9, no. 1, pp. 1153–1165, 2023.

[5] B.-M. Nguyen, J. P. F. Trovao, and M. C. Ta, "Double-layer energy management for multi-motor electric vehicles," *IEEE Transactions on Vehicular Technology*, vol. 72, no. 7, pp. 8623–8635, 2023.

[6] Y. Teshima, N. Hirakoso, Y. Shigematsu, Y. Hirama, and H. Kawabata, "Optimal driving strategy for solar electric vehicle," *IEEJ Journal of Industry Applications*, vol. 10, no. 3, pp. 303–309, 2021.

[7] M. Hattori, O. Shimizu, S. Nagai, H. Fujimoto, K. Sato, Y. Takeda, and T. Nagashio, "Quadrant dynamic programming for optimizing velocity of ecological adaptive cruise control," *IEEE/ASME Transactions on Mechatronics*, vol. 27, no. 3, pp. 1533–1544, 2022.

[8] E. Ozatay, U. Ozguner, D. Filev, and J. Michelini, "Analytical and numerical solutions for energy minimization of road vehicles with the existence of multiple traffic lights," in *52nd IEEE Conference on Decision and Control*, 2013, pp. 7137–7142.

[9] B. Liu, C. Sun, B. Wang, and F. Sun, "Adaptive speed planning of connected and automated vehicles using multi-light trained deep reinforcement learning," *IEEE Transactions on Vehicular Technology*, vol. 71, no. 4, pp. 3533–3546, 2022.

[10] A. Alessandrini, A. Campagna, P. D. Site, F. Filippi, and L. Persia, "Automated vehicles and the rethinking of mobility and cities," *Transportation Research Procedia*, vol. 5, pp. 145–160, 2015, sIDT Scientific Seminar 2013. [Online]. Available: https://www.sciencedirect.com/science/article/pii/S2352146515000034

[11] H. Nakamura, M. Iryo-Asano, and T. Oguchi, "10 - japan," in *Global Practices on Road Traffic Signal Control*, K. Tang, M. Boltze, H. Nakamura, and Z. Tian, Eds. Elsevier, 2019, pp. 163–184. [Online]. Available: https://www.sciencedirect.com/science/article/pii/B9780128153024000108

[12] G. Mahler and A. Vahidi, "An optimal velocity-planning scheme for vehicle energy efficiency through probabilistic prediction of traffic-signal timing," *IEEE Transactions on Intelligent Transportation Systems*, vol. 15, no. 6, pp. 2516–2523, 2014.

[13] Z. Wang, M. Dridi, and A. E. Moudni, "Data-driven trajectory planning strategy for connected vehicles at signalized intersection," in *2022 17th International Conference on Control, Automation, Robotics and Vision (ICARCV)*, 2022, pp. 111–118.

[14] A. S. M. Bakibillah, M. A. S. Kamal, C. P. Tan, T. Hayakawa, and J.-I. Imura, "Event-driven stochastic eco-driving strategy at signalized intersections from self-driving data," *IEEE Transactions on Vehicular Technology*, vol. 68, no. 9, pp. 8557–8569, 2019.

[15] A. S. M. Bakibillah, M. A. S. Kamal, and C. P. Tan, "Sustainable eco-driving strategy at signalized intersections from driving data," in *2020 59th Annual Conference of the Society of Instrument and Control Engineers of Japan (SICE)*, 2020, pp. 165–170.

[16] ITS Division, National Institute for Land and Infrastructure Management, "ETC2.0:"ETC2.0" Probe information," http://www.nilim.go.jp/lab/qcg/research/etc-2.0_en.html, Accessed 27 Nov. 2022.

[17] Y. Hosomi, S. Yamada, B.-M. Nguyen, S. Nagai, and H. Fujimoto, "Basic study on energy-optimized speed trajectory for electric vehicles between traffic signals based on stochastic model using low frequency floating car data," in *IEEJ International Workshop on Sensing, Actuation, Motion Control, and Optimization*, 2023, pp. 1–6.